Wan Ahmad Kamil, W. N. I., Takebayashi, Y., Findlay, J., Heesom, K. J., Jiménez-Castellanos, J. C., Zhang, J., Graham, L., Bowker, K., Williams, O. M., MacGowan, A. P., & Avison, M. B. (2018). Prediction of fluoroquinolone susceptibility directly from whole-genome sequence data by using liquid chromatography-tandem mass spectrometry to identify mutant genotypes. *Antimicrobial Agents and Chemotherapy*, *62*(3), e01814-01817. https://doi.org/10.1128/AAC.01814-17

Peer reviewed version

Link to published version (if available):
10.1128/AAC.01814-17

Prediction of fluoroquinolone susceptibility directly from whole genome sequence data using liquid chromatography-tandem mass spectrometry to identify mutant genotypes.

Running Title: Predicting fluoroquinolone susceptibility.

Wan Ahmad Kamil WAN NUR ISMAH,[1,2] Yuiko TAKEBAYASHI,[1] Jacqueline FINDLAY,[1] Kate J. HEESOM,[3] Juan-Carlos JIMÉNEZ-CASTELLANOS,[1] Jay ZHANG,[1] Lee GRAHAM,[4] Karen BOWKER,[4] O. Martin WILLIAMS,[4] Alasdair P. MacGOWAN,[1,4] and Matthew B. AVISON[1*].

[1]School of Cellular & Molecular Medicine, University of Bristol, Bristol. UK

[2]Faculty of Biotechnology & Biomolecular Sciences, Universiti Putra Malaysia, Selangor Darul Ehsan, Malaysia

[3]Bristol Proteomics Facility, University of Bristol, UK

[4]Department of Infection Sciences, Severn Infection Partnership, Southmead Hospital, Bristol, UK.

***Correspondence: Matthew B. Avison, School of Cellular & Molecular Medicine, Biomedical Sciences Building, University Walk, Bristol. BS81TD. UK. bimba@bris.ac.uk. +44(0)1173312035.**

ABSTRACT

Fluoroquinolone resistance in Gram-negative bacteria is multifactorial, involving target site mutations, reductions in fluoroquinolone entry due to reduced porin production, increased fluoroquinolone efflux, enzymes that modify fluoroquinolones, and Qnr, a DNA mimic that protects the drug target from fluoroquinolone binding. Here we report a comprehensive analysis using transformation and in vitro mutant selection, of the relative importance of each of these mechanisms in fluoroquinolone non-susceptibility, using *Klebsiella pneumoniae* as a model system. Our improved biological understanding was then used to generate 47 rules that can predict fluoroquinolone susceptibility in *K. pneumoniae* clinical isolates. Key to the success of this predictive process was the use of liquid chromatography tandem mass spectrometry to measure the abundance of proteins in extracts of cultured bacteria, identifying which sequence variants seen in the whole genome sequence data were functionally important in the context of fluoroquinolone susceptibility.

INTRODUCTION

The use of whole genome sequencing (WGS) to predict antibacterial drug susceptibility/non-susceptibility in the clinical setting has recently been subject to a subcommittee report from the European Committee on Antimicrobial Susceptibility Testing (1). Aside from issues around universal WGS data availability and quality, particularly regarding clinical samples with low bacterial titres, the committee considered that a lack of basic biological understanding of antibacterial resistance (ABR) mechanisms was slowing down progress in this area (1). There have been some successes predicting susceptibility/non-susceptibility direct from WGS in key Gram-negative human pathogens such as *Escherichia coli* and *Klebsiella pneumoniae* carrying well-known plasmid encoded ABR mechanisms, or commonly encountered antibacterial target site mutations (2, 3). However, when ABR is multi-factorial, as typified by fluoroquinolone resistance, prediction of susceptibility/non-susceptibility is more difficult (1, 4).

Fluoroquinolones have a fluorine atom attached to the central quinolone ring system (5–7). They have a broad spectrum of activity against both Gram-negative and Gram-positive bacteria and play an important role in clinical applications (8–10). Their mode of action involves binding to type II DNA topoisomerases, GyrA/B and ParC/E, resulting in lethal double strand breaks in DNA (8, 11). A single point mutation in the quinolone resistance-determining region (QRDR) of GyrA confers nalidixic acid resistance in *E. coli* but additional factors are required for fluoroquinolone resistance. For example, QRDR mutations in ParC, a secondary target of fluoroquinolones (12) or mutations in the transcriptional repressor gene, *ramR*, which leads to over-production of the resistance nodulation cell division (RND) family efflux pump AcrAB-TolC (13–16). Over-production of OqxAB, another chromosomally-

encoded RND efflux pump that probably works with TolC, also confers reduced fluoroquinolone susceptibility in *K. pneuomoniae*, and results from mutations in the transcriptional repressor gene *oqxR* (17).

When encoded on a plasmid in *E. coli*, *oqxAB* also confers fluoroquinolone resistance via drug efflux (18, 19). Other plasmid-mediated quinolone resistance (PMQR) genes include *qnrA* (20), which encodes a pentapeptide repeat protein that protects GyrA from inhibition by fluoroquinolones, reducing susceptibility. Other *qnr* gene families: *qnrB* (21) *qnrC* (22) *qnrS* (23) and *qnrD* (24) are commonly seen in clinical Enterobacteriaceae isolates, as is the PMQR gene *aac-6'-Ib*-cr, encoding an aminoglycoside acetyltransferase capable of acetylating fluoroquinolones at the amino nitrogen if they have a piperazinyl substituent, e.g. ciprofloxacin (25).

Our aim in performing the work set out below was to complete an extensive analysis of the individual and combined contributions of these known mechanisms to fluoroquinolone non-susceptibility in *K. pneumoniae* using sequential mutant selection and transformation, with LC-MS/MS proteomics being used to monitor protein production and DNA sequencing being used to identify mutations. Our aim was to generate a series of "rules" that might be applied to WGS data to predict fluoroquinolone susceptibility in *K. pneumoniae*. We then tested our rules against 40 *K. pneumoniae* clinical isolates.

MATERIALS AND METHODS

Bacterial strains and antibacterial drug susceptibility testing

The isogenic pair *K. pneumoniae* Ecl8 (26) and Ecl8Δ*ramR* (27) were used throughout. Forty human *K. pneumoniae* clinical isolates were studied. Details of these isolates are given in **Table S1**. Disc susceptibility testing was performed and minimum inhibitory concentrations (MICs) were determined according to CLSI methodologies (28, 29). Susceptibility/non-susceptibility was interpreted using CLSI performance standards (30).

Selection of in vitro K. pneumoniae mutants conferring reduced fluoroquinolone susceptibility and transformation with PMQR genes

Mutants were generated by plating 100 µl of an overnight culture on LB agar containing ciprofloxacin or nalidixic acid at various doubling concentrations below the CLSI defined non-susceptibility breakpoint. First step mutants were then re-selected using increasing concentrations of ciprofloxacin to generate fluoroquinolone non-susceptible mutants. PCR-sequencing to identify mutations was performed using primers listed in **Table S2**. The PMQR genes *qnrA1* and *aac(6')-Ib-cr*, were synthesised (Eurofins Genomics) as defined in **Table S2** to include native promoters and ligated into the pEX-K4 cloning vector (Eurofins). Recombinant plasmids were used to transform *K. pneumoniae* to kanamycin (30 mg/L) resistance using electroporation as standard for laboratory-strain *E. coli.*

Quantitative analysis of whole cell proteome via Orbitrap LC-MS/MS and qRT-PCR.

Cells were cultured in 50 ml nutrient broth (Oxoid) with shaking (160 rpm) at 37^{o}C until the optical density at 600 nm (OD_{600}) reached 0.5-0.7. RNA was purified, and qRT-PCR was performed as previously described (31, 32). For proteomics, cells in cultures were pelleted

by centrifugation (10 min, 4,000 × g, 4˚C) and resuspended in 20 mL of 30 mM Tris-HCl, pH 8 and broken by sonication with a cycle of 1 sec on, 0.5 sec off for 3 min at amplitude of 63% using a Sonics Vibracell VC-505TM (Sonics and Materials Inc., Newton, Connecticut, USA). Following centrifugation (15 min, 4°C, 8,000 rpm, Sorval RC5B with SS34 rotor), the protein concentration in the supernatant was quantified using Biorad Protein Assay Dye Reagent Concentrate according to the manufacturer's instructions. One microgram of total protein was separated by SDS-PAGE using 11% acrylamide, 0.5% bis-acrylamide (Biorad) gels and a Biorad Min-Protein Tetracell chamber model 3000X1. Gels were run at 200 V until the dye front had moved approximately 1 cm into the separating gel. Proteins in gels were stained with Instant Blue (Expedeon) for 20 min and de-stained in water.

The one centimetre of gel lane containing protein was cut out and proteins subjected to in-gel tryptic digestion using a DigestPro automated digestion unit (Intavis Ltd). The resulting peptides were fractionated using an Ultimate 3000 nanoHPLC system in line with an LTQ-Orbitrap Velos mass spectrometer (Thermo Scientific) according to our previously published protocol (31, 32). The raw data files were processed and quantified using Proteome Discoverer software v1.4 (Thermo Scientific) and searched against the UniProt *K. pneumoniae* strain ATCC 700721 / MGH 78578 database (5126 protein entries; UniProt accession 272620) using the SEQUEST (Ver. 28 Rev. 13) algorithm. Protein Area measurements were calculated from peptide peak areas using the Top 3 method (33) and were then used to calculate the abundance of each protein. Proteins with fewer than three peptide hits were excluded from the analysis. Raw protein abundance for each protein was divided by the average abundance of a ribosomal protein to normalise for sample to sample loading variability.

Fluorescent Hoechst (H) 33342 dye accumulation assay

Envelope permeability was estimated as described previously (31, 32) in bacteria grown in Cation Adjusted Muller-Hinton Broth (Sigma) using an established fluorescent dye accumulation assay (34). H33342 dye (Sigma) was used at a final concentration of 2.5 µM.

Whole genome sequencing and data analysis

Genomes were sequenced by MicrobesNG (Birmingham, UK) on a HiSeq 2500 instrument (Illumina, San Diego, CA, USA). Reads were trimmed using Trimmomatic (35) and assembled into contigs using SPAdes 3.10.1 (http://cab.spbu.ru/software/spades/). The presence of resistance genes was determined using MLST 1.8, PlasmidFinder (36) and ResFinder 2.1 (37), and on the Center for Genomic Research platform (https://cge.cbs.dtu.dk/services/). Assembled contigs were mapped to reference genome *K. pneumoniae* Ecl8 (GCA_000315385.1) obtained from GenBank using progressive Mauve alignment software (38).

RESULTS & DISCUSSION

Fluoroquinolone non-susceptibility in K. pneumoniae requires combinations of different mechanisms

A total of 192 mutants with reduced fluoroquinolone susceptibility were generated from *K. pneumoniae* Ecl8 and Ecl8Δ*ramR*. Among the 29 representative mutants that were extensively characterised, 16 had quinolone target site mutations in *gyrA* clustered into four different alleles, each encoding a single amino acid substitution within the QRDR: Ser83Phe, Ser83Tyr, Asp87Tyr or Gly81Cys. Multiple mutations in *gyrA* or mutations in other

topoisomerase genes, e.g. *parC* were not identified. Mutations in known regulators of drug efflux were also seen. OqxR mutations were found in 12/29 fully characterised mutants, including frameshift mutations and nonsense and missense mutations at various positions (**Table S3**). In contrast, only a single (Thr124Pro) RamR mutation was found, and no mutations in AcrR were identified. The roles of two PMQR genes were also assessed: *qnr* (represented by the *qnrA1* variant) and *aac(6')-Ib-cr*, both being provided on a vector with expression driven by their native promoters.

No single acquisition event; whether GyrA mutations, RamR or OqxR mutations, or carriage of a PMQR conferred clinically relevant ciprofloxacin non-susceptibility in *K. pneumoniae* Ecl8. Combinations of an *oqxR* or *ramR* plus a *gyrA* mutation or of an *oqxR* or *ramR* mutation plus carriage of *qnr* were the only double combinations that conferred ciprofloxacin non-susceptibility. In 10 triple and five quadruple combinations tested, all conferred fluoroquinolone non-susceptibility except the *ramR*/*oqxR* double mutant plus *aac(6')-Ib-cr* (**Table S4**).

Predicting fluoroquinolone susceptibility in K. pneumoniae clinical isolates from WGS

The results from *in vitro K. pneumoniae* Ecl8 mutant and transformant characterisation (**Table S4**) were used to generate a set of 31 rules to predict fluoroquinolone susceptibility/non-susceptibility in *K. pneumoniae* as shown in **Table S5**. The 31 rules were then applied to 10 *K. pneumoniae* clinical isolates based on WGS data. The presence of PMQR genes was defined as a binary result from the WGS data, given that all genes were fully intact. The presence of QRDR mutations in GyrA and of SNPs affecting the amino acid sequence of RamR and OqxR were read directly from the WGS data. To confirm whether the identified regulatory SNPs activated efflux pump production in these clinical isolates, whole

cell LC-MS/MS proteomics was performed. Clinical isolates carrying Thr141Ile and 194K insertion mutations in RamR (6/10 clinical isolates carrying one or both) did not hyperproduce AcrA and AcrB (**Table 1**), as would be expected from a true RamR loss of function mutation (32), so these variants were considered functionally wild-type, and to have arisen by random genetic drift. Two out of 10 isolates carried OqxR mutations, and both were confirmed to hyperproduce OqxB (**Table 1**).

Applying our predictive rules (**Table S5**), WGS information for the 10 clinical isolates, with proteomics being used to confirm/deny suspected *oqxR*/*ramR* loss of function mutations, allowed correct prediction of ciprofloxacin susceptibility/non-susceptibility in 7/10 isolates. The three remaining isolates were incorrectly predicted to be ciprofloxacin susceptible as defined by Rule 15, which is production of Qnr and Aac-6'-Ib-cr in an otherwise wild-type background (**Table S5**). The Rule 15 clinical isolates were in fact ciprofloxacin non-susceptible, though they were susceptible to all other fluoroquinolones tested (**Table 1**).

Clinical isolates with low OmpK35:OmpK36 porin ratios have reduced fluoroquinolone susceptibility

We hypothesised that the three "Rule 15" clinical isolates incorrectly predicted to be fluoroquinolone susceptible (**Table 1**) have reduced envelope permeability compared with Ecl8, the isolate used to define our predictive rules (**Table S4, S5**). Fluorescent dye accumulation assays revealed that the shape of the dye accumulation curve for representative Rule 15 clinical isolates KP7 and KP8 (**Fig. 1A, B**) was like that seen previously upon *micF* overexpression in Ecl8, i.e. causing reduced OmpF (OmpK35) porin production (32). Porin reduction retards entry of the dye but does not prevent accumulation of the dye over time. This phenotype is in stark contrast to efflux mediated reduced envelope

permeability, which gives a persistent level of reduced dye accumulation, as seen in the Ecl8Δ*ramR* mutant previously (32), and, for example, in clinical isolate KP21, having a *ramR* mutation and over-producing AcrAB-TolC (**Table 2, Fig. 1C**).

During growth in the same medium used to perform the proteomic analyses on our clinical isolates (nutrient broth), the OmpF:OmpC ratio seen in Ecl8 was approximately 1:1 (32). For these 10 test clinical isolates, the OmpF:OmpC ratio was in a range of 0.25:1 to 0.40:1, or it was zero due to apparent loss of OmpF (**Table 1**). This observed reduced OmpF:OmpC ratio in the clinical isolates relative to Ecl8 rationalised the observed envelope permeability assay data (**Fig. 1**) and supported our hypothesis that clinical Rule 15 isolates have reduced OmpF porin levels compared with Ecl8, creating a ciprofloxacin non-susceptible phenotype in the presence of Qnr and Aac-6'-Ib-cr.

Following analysis of an additional 30 *K. pneumoniae* clinical isolates, proteomics revealed that all the clinical isolates in our collection have an OmpF:OmpC ratio of <0.5 (**Table 2**), so, we predicted that these clinical isolates also have reduced envelope permeability compared with Ecl8. This proved to be correct, e.g. for representative isolate KP46, where the dye accumulation curve was like that for the Rule 15 clinical isolates (**Fig. 1A, 1B, 1D)**.

Based on this finding of reduced OmpF:OmpC ratio in the clinical isolates relative to Ecl8, we set out to refine our predictive rules (**Table S5**), defined using Ecl8, to take this reduced permeability into consideration. Comparisons between the MICs of ciprofloxacin against Ecl8 variants and equivalent clinical isolates (having reduced OmpF:OmpC ratios) were possible for Rule 4 (*qnr*): 0.063 mg.L^{-1} for Ecl8 vs 0.25 mg.L^{-1} for KP1; Rule 5 (*aac-6'-Ib-cr*): 0.016 mg.L^{-1} for Ecl8 vs for 0.063 mg.L^{-1} for KP34; Rule 15 (*qnr* plus *aac-6'-Ib-cr*): 0.5 mg.L^{-1} for Ecl8 vs 2 mg.L^{-1} for KP8; Rule 21 (*gyrA* plus *qnr* plus *aac-6'-Ib-cr*): 2 mg.L^{-1} for Ecl8 vs 8

mg.L^{-1} for KP6. Based on the finding that in each case the reduced OmpF:OmpC ratio increases the MIC of ciprofloxacin by 4-fold, we modified our predictive rules. To do this, we first determined the ciprofloxacin MIC against the 12/31 ciprofloxacin susceptible Ecl8 derivatives (**Table S5**) and applied a 4-fold MIC increase correction to account for reduced permeability (RP) caused by a reduced background OmpF:OmpC ratio. In this way, 5/31 of the originally defined predictive rules were altered to predict ciprofloxacin non-susceptibility based on MIC breakpoints after applying this RP correction (**Table S5**).

The impact of multiple QRDR mutations on fluoroquinolone susceptiblity

Following application of the revised rules, allowing for an OmpF:OmpC ratio of <0.5 (**Table S5**), we were successful in predicting ciprofloxacin susceptibility/non-susceptibility in 29/30 additional clinical isolates not previously tested (**Table 2**). To understand the incorrect prediction of ciprofloxacin susceptibly in isolate KP17 (predictive Rule 1RP), we considered additional mechanisms that might be involved. We noted from the WGS data that isolate KP17 carries both a GyrA and a ParC topoisomerase mutation, never seen in our Ecl8 mutants, and so not included in our 31 predictive rules, but relatively common in our clinical isolates (**Table 1, 2**). To assess the impact of a second QRDR mutation we compared ciprofloxacin MICs against clinical isolates having a single or double QRDR but otherwise defined by the same predictive rule. For example, the ciprofloxacin MIC against KP6 (rule 21, one QRDR mutation) was 8 mg.L^{-1} and the MIC against KP3 (rule 21, two QRDR mutations) was four-fold higher: 32 mg.L^{-1}. Applying this 4-fold MIC correction to the predicted MIC of ciprofloxacin against a single QRDR mutant Rule 1RP isolate (1 mg.L^{-1}, susceptible) (**Table S5**), led to a predicted ciprofloxacin MIC against a double QRDR mutant of 4 mg.L^{-1} (non-susceptible, now correctly predicting the observed phenotype of KP17) (**Table 2**). We have

therefore added additional predictive rules to consider the existence of double GyrA or GyrA/ParC QRDR mutations, making 47 rules in total (**Table S6**).

Mutations in repressor binding sites upregulate efflux pump production and influence fluoroquinolone susceptibility.

During our analysis, we noticed that, whilst clinical isolate KP27 has a wild-type *ramR* sequence, the proteomics data showed that it hyper-produces AcrAB (**Table 2**). This was confirmed using qRT-PCR for *acrA* relative to a wild-type control isolate, KP47, but *ramA* was not over-expressed in KP27, validating the observation that RamR is wild-type (**Fig. 2A, B, Table 2**) (32). WGS identified a mutation in the *acrR-acrA* intergenic region in KP27, causing a T-C transition at the 5th position of the first AcrR binding motif (5'TACA**T**ACATT3') (**Fig. 2C**), predicted to de-repress *acrAB* expression (39). Whilst it does not affect our designation of KP27 as ciprofloxacin non-susceptible, this example shows how LC-MS/MS can allow the identification of previously unknown regulatory mutations involved in phenotypically relevant efflux pump over-production.

CONCLUSIONS

We have demonstrated step-wise combinations of mechanisms leading to fluoroquinolone non-susceptibility in *K. pneumoniae*, as well as characterising the importance of each mechanism and the interplay between them. Using this information, we have successfully applied WGS to predict ciprofloxacin susceptibility/non-susceptibility in *K. pneumoniae* clinical isolates. However, LC-MS/MS proteomics was essential for this process, and particularly for determining the relative importance of different SNPs seen in the efflux

pump regulators OqxR and RamR. The more phenotypically relevant SNPs we can identify (e.g. see **Table S3** for a list of OqxR loss of function mutations uncovered here) the more we will be able to rely on WGS alone to identify phenotypically relevant mutations.

LC-MS/MS also allowed us to uncover new biology in this study. We incorrectly predicted ciprofloxacin susceptibility in genotypically Rule 15 clinical isolates, a particularly common group, because they have reduced envelope permeability compared with Ecl8. LC-MS/MS revealed that this is due to downregulation of OmpF, and a consequent reduction in the OmpF:OmpC porin ratio. In fact, it would seem likely that this difference is due to a genetic change in Ecl8, rather than an equivalent genetic change in all the clinical isolates, so we would propose that the predictive rules listed in **Table S6**, which allow for this reduced OmpF:OmpC ratio, are appropriate to use for all clinical isolates. Allowing for GyrA/ParC double mutations expanded the non-wild-type rules to a total number of 47 of which only 7 predict ciprofloxacin susceptibility.

Overall, this work as enhanced our biological understanding of fluoroquinolone resistance in *K. pneumoniae* and will improve our ability to predict ciprofloxacin susceptibility in clinical isolates based on WGS data. Particularly, it shows the value of using proteomics to clarify genotype to phenotype relationships, and to bridge the gap between WGS and antimicrobial susceptibility testing where mechanisms of resistance are multi-factorial and complex.

Acknowledgements

Genome sequencing was provided by MicrobesNG (http://www.microbesng.uk), which is supported by the BBSRC (grant number BB/L024209/1).

Funding

This work was funded by grant MR/N013646/1 to M.B.A., A.P.McG., O.M.W. and K.J.H. and grant NE/N01961X/1 to M.B.A. and A.P.McG. from the Antimicrobial Resistance Cross Council Initiative supported by the seven research councils. W. A. K W. N. I. was funded by a postgraduate scholarship from the Malaysian Ministry of Education. JC-JC was funded by a postgraduate scholarship from CONACyT, Mexico.

Transparency Declaration

None to declare – All authors.

FIGURE LEGENDS

Figure 1: The accumulation of H33342 dye over a 30 cycle (45 minute) incubation period by *K. pneumoniae* clinical isolates: (A) KP7, (B) KP8, (C) KP21, (D) KP46. In each case, permeability was compared with Ecl8 (set to 100%) in cells grown in MHB. Each line shows mean data for three biological replicates with 8 technical replicates in each and error bars define the standard error of the mean (SEM).

Figure 2: Expression of (A) *acrA* and (B), *ramA* in *K. pneumoniae* clinical isolates KP21 (*ramR* mutant) and KP27 (*ramR* wild-type) both normalised to expression in a control isolate KP17, using qRT-PCR. Data are presented as means +/- SEM, *n*=3 preparations of RNA (C) shows that a single nucleotide polymorphism is present in the putative AcrR binding site upstream of *acrAB* in KP27.

FIGURES

Figure 1

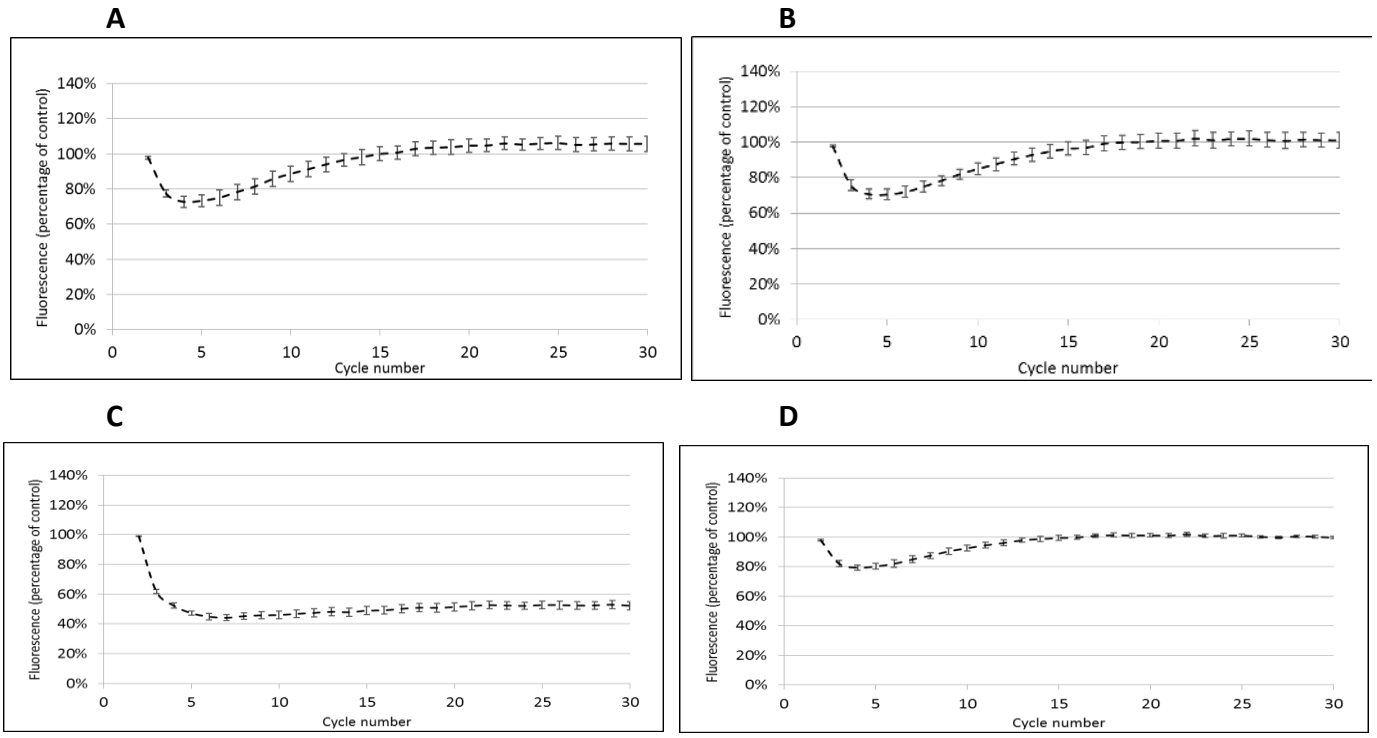

Figure 2

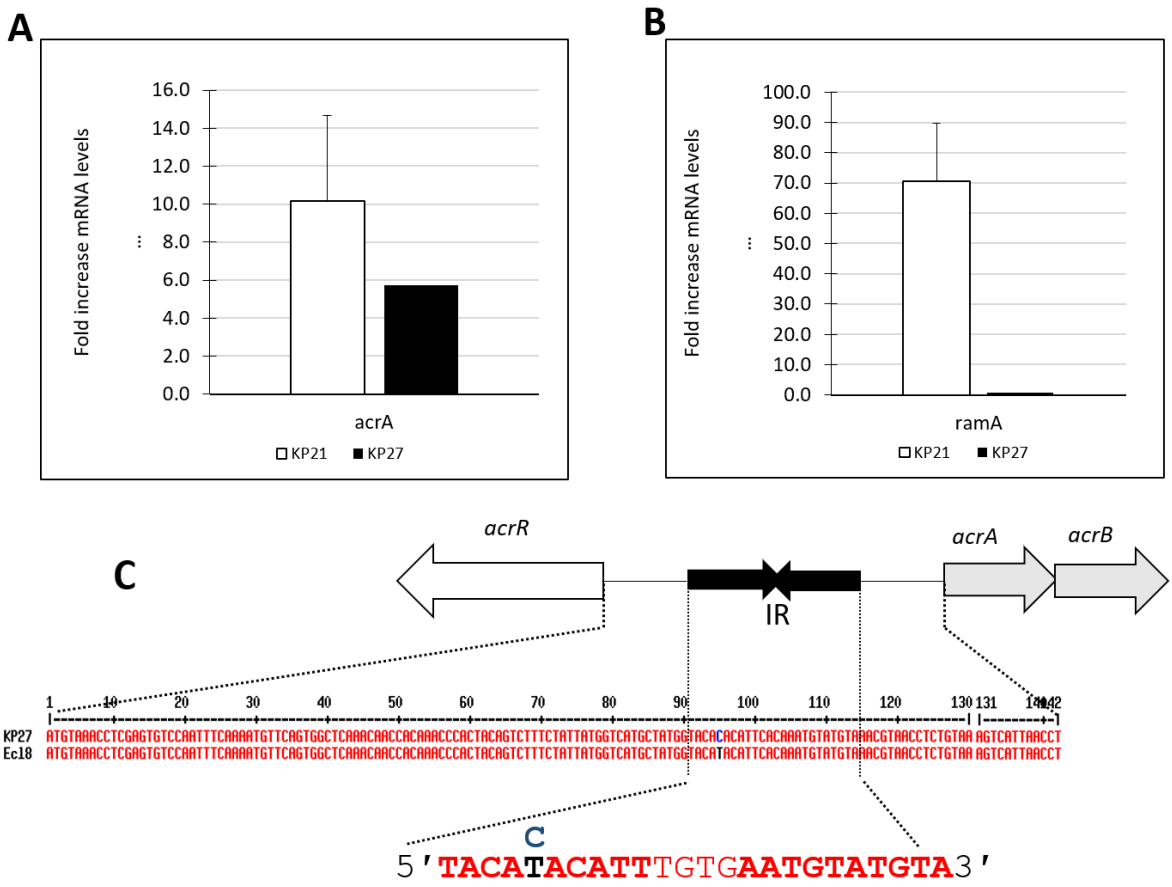
A
Fold increase mRNA levels
16.0
14.0
12.0
10.0
8.0
6.0
4.0
2.0
0.0
acrA
KP21
KP27
B
Fold increase mRNA levels
100.0
90.0
80.0
70.0
60.0
50.0
40.0
30.0
20.0
10.0
0.0
ramA
KP21
KP27
C
acrR
IR
acrA
acrB
KP27 ATGTAAACCTCGAGTGTCCAATTTCAAAATGTTCAGTGGCTCAAACAACCACAAACCCACTACAGTCTTTCTATTATGGTCATGCTATGGTACACACATTCACAAATGTATGTAAACGTAACCTCTGTAA AGTCATTAACCT
Ec18 ATGTAAACCTCGAGTGTCCAATTTCAAAATGTTCAGTGGCTCAAACAACCACAAACCCACTACAGTCTTTCTATTATGGTCATGCTATGGTACATACATTCACAAATGTATGTAAACGTAACCTCTGTAA AGTCATTAACCT
C
5'TACATACATTTGTGAATGTATGTA3'

Table 1: Combination of disc test, proteomics, WGS and predictions of fluoroquinolone susceptibility for *K. pneumoniae* clinical isolates

Isolate	GyrA	OqxR	OqxB	RamR	AcrA, B	*qnr*	*aac(6')-Ib-cr*	Prediction	CIP	LEV	NOR	OFL	ParC	OmpF:OmpC ratio
	Mutation	Mutation	Abundance	Mutation	Abundance	Presence	Presence	(Rule)	Zone	Zone	Zone	Zone	Mutation	
KP1	-	-	ND	-	0.07, 0.04	S	-	S (4)	S	S	S	S	-	0.30
KP2	-	-	ND	*Thr141Ile	0.10, 0.03	B, S	+	S (15)	NS	S	S	S	-	0.28
KP3	Ser83Ile	-	ND	*Thr141Ile	0.11, 0.03	B	+	NS (21)	NS	NS	NS	NS	Ser80Ile	0.00
KP4	Ser83Tyr Asp87Gly	-	ND	**Lys9Ile** *Thr141Ile	**0.26, 0.2**	S	-	NS (19)	NS	NS	NS	NS	Ser80Ile	0.00
KP5	-	***oqxR* deleted**	**0.23**	*Thr141Ile *194K	0.08, 0.07	-	-	S (2)	S	S	S	S	-	0.28
KP6	Ser83Tyr	-	ND	-	0.10, 0.03	B	+	NS (21)	NS	S	NS	NS	-	0.25
KP7	-	-	ND	-	0.13, 0.06	B	+	S (15)	NS	S	S	S	-	0.25
KP8	-	-	ND	*Thr141Ile	0.13, 0.04	B	+	S (15)	NS	S	S	S	-	0.25
KP9	Ser83Phe Asp87Ala	**Glu24STOP**	**0.06**	*ramR*/*ramA* deleted	0.08, 0.03	-	-	NS (6)	NS	NS	NS	NS	Ser80Ile	0.40
KP10	Ser83Ile	-	ND	*Thr141Ile	0.10, 0.02	B	+	NS (21)	NS	NS	NS	NS	Ser80Ile	0.26

CIP: Ciprofloxacin; LEV: Levofloxcin; NOR: Norfloxacin; OFL; Ofloxacin

Susceptibilities were defined by reference to zone diameters that were the means of three repetitions rounded to the nearest integer.

Zones shaded blue are non-susceptible according to susceptibility breakpoints set by the CLSI (30).

Predictions shaded green and red show success and failure in predicting fluoroquinolone susceptibility using the preliminary rules (Table S5).

*Changes in amino acid not associated with changes in gene function, likely due to genetic drift.

+; gene is present, -; mutations not detected or gene is absent, ND; protein not detected.

Table 2: Combination of disc test, proteomics, genome sequencing and predictions of fluoroquinolone susceptibility for *K. pneumoniae* clinical isolates

Isolate	GyrA Mutation	ParC Mutation	OqxR Mutation	OqxB Abundance	RamR Mutation	AcrA, B Abundance	*qnr* Presence	*aac(6')-Ib-cr* Presence	OmpF:OmpC ratio	Prediction (Rule)	CIP (5) Zone	LEV (5) Zone	NOR (10) Zone	OFL (5) Zone
KP11	Ser83Ile	Ser80Ile	-	ND	*Thr141Ile **Met184Val** *194K	**0.24, 0.09**	S	-	0.00	NS (19RP)	NS	NS	NS	NS
KP12	Ser83Ile	Ser80Ile	**Asp3Tyr**	**0.11**	*Thr141Ile	0.14, 0.04	-	-	0.00	NS (6RP)	NS	NS	NS	NS
KP13	Ser83Ile	Ser80Ile	-	ND	**Lys63FS**	**0.39, 0.2**	B, S	+	0.00	NS (29RP)	NS	NS	NS	NS
KP14	-	-	-	ND	*ramR/ramA* deleted	0.09, 0.04	B	+	0.36	NS (15RP)	NS	S	S	S
KP15	-	-	-	ND	-	0.14, 0.03	S	+	0.21	NS (15RP)	NS	S	S	S
KP16	Ser83Ile	Ser80Ile	-	ND	*Thr141Ile	0.11, 0.03	S	-	0.40	S (8RP)	NS	NS	NS	NS
KP17	Ser83Ile	Ser80Ile	-	ND	*Thr141Ile	0.11, 0.04	-	-	0.35	S (1RP)	NS	S	NS	NS
KP18	-	-	-	ND	*Ala19Val *Thr141Ile	0.12, 0.05	S	+	0.36	NS (15RP)	NS	S	S	S
KP19	-	-	-	ND	*Thr141Ile *194K	0.1, 0.03	B	+	0.42	NS (15RP)	NS	S	S	S
KP20	-	-	**Ala19Val**	**0.08**	*Thr141Ile	0.11, 0.04	B	-	0.00	NS (11RP)	NS	NS	NS	NS
KP21	-	-	-	ND	**Arg44FS**	**0.41, 0.23**	S	-	0.00	NS (13RP)	NS	NS	NS	NS
KP22	-	-	-	ND	*Thr141Ile *194K	0.09, 0.06	B	+	0.45	NS (15RP)	NS	S	S	S
KP23	-	-	-	ND	*Thr141Ile *194K	0.05, 0.03	B	+	0.41	NS (15RP)	NS	S	S	S

KP24	-	-	-	ND	-	0.13, 0.07	B	+	0.34	NS (15RP)	NS	S	S	S
KP25	-	-	-	ND	*Thr141Ile	0.12, 0.09	B	+	0.29	NS (15RP)	NS	S	S	S
KP26	-	-	-	ND	*Thr141Ile	0.08, 0.02	B	+	0.33	NS (15RP)	NS	S	S	S
KP27	Ser83Tyr Asp87Phe	Ser80Ile	-	ND	*Thr141Ile	**0.36, 0.15**	-	+	0.00	NS (9RP†)	NS	NS	NS	NS
KP28	-	-	**Leu76FS**	**0.13**	*Thr141Ile	0.12, 0.04	S	-	0.00	NS (11RP)	NS	NS	NS	NS
KP30	Ser83Ile	Ser80Ile	**Val130Ala**	**0.14**	**Ala40Val** *Thr141Ile *194K	**0.87, 0.33**	-	-	0.00	NS (16RP)	NS	NS	NS	NS
KP31	-	-	-	ND	*Thr141Ile	0.08, 0.04	-	-	0.43	S (WT)	S	S	S	S
KP32	-	-	-	ND	-	0.08, 0.04	-	-	0.40	S (WT)	S	S	S	S
KP33	-	-	-	ND	*Thr141Ile	0.08, 0.03	-	-	0.37	S (WT)	S	S	S	S
KP34	-	-	-	ND	*Thr141Ile	0.16, 0.07	-	+	0.36	S (5RP)	S	S	S	S
KP38	-	-	-	ND	*Thr141Ile	0.05, 0.31	-	-	0.00	S (WT)	S	S	S	S
KP40	-	-	-	ND	*Ala19Val *Thr141Ile	0.03, 0.03	-	-	0.36	S (WT)	S	S	S	S
KP46	-	-	-	ND	-	0.03, 0.01	-	-	0.34	S (WT)	S	S	S	S
KP47	-	-	-	ND	-	0.10, 0.04	-	-	0.32	S (WT)	S	S	S	S
KP48	-	-	-	ND	-	0.08, 0.04	-	-	0.35	S (WT)	S	S	S	S
KP50	-	-	-	ND	*Ile106Ser *Thr141Ile	0.05, 0.03	-	-	0.45	S (WT)	S	S	S	S
KP59	-	-	-	ND	**Thr50Ala**	**0.21, 0.11**	-	-	0.41	S (3RP)	S	S	S	S

CIP: Ciprofloxacin; LEV: Levofloxcin; NOR: Norfloxacin; OFL; Ofloxacin

Susceptibilities were defined by reference to zone diameters that were the means of three repetitions rounded to the nearest integer.

Zones shaded blue are non-susceptible according to susceptibility breakpoints set by the CLSI (30).

Predictions shaded green and red show success and failure in predicting fluoroquinolone susceptibility using the RP rules (Table S5).

*Changes in amino acid not associated with changes in gene function, likely due to genetic drift; † KP27 is an AcrAB over-producer – see text.

+; gene is present, -; mutations not detected or gene is absent, ND; protein not detected.

References

1. Ellington MJ, Ekelund O, Aarestrup FM, Canton R, Doumith M, Giske C, Grundman H, Hasman H, Holden MTG, Hopkins KL, Iredell J, Kahlmeter G, Köser CU, MacGowan A, Mevius D, Mulvey M, Naas T, Peto T, Rolain J-M, Samuelsen Ø, Woodford N. 2017. The role of whole genome sequencing in antimicrobial susceptibility testing of bacteria: report from the EUCAST Subcommittee. Clin Microbiol Infect 23:2–22.

2. Stoesser N, Batty EM, Eyre DW, Morgan M, Wyllie DH, Del Ojo Elias C, Johnson JR, Walker AS, Peto TEA, Crook DW. 2013. Predicting antimicrobial susceptibilities for *Escherichia coli* and *Klebsiella pneumoniae* isolates using whole genomic sequence data. J Antimicrob Chemother 68:2234–2244.

3. Zankari E, Hasman H, Cosentino S, Vestergaard M, Rasmussen S, Lund O, Aarestrup FM, Larsen M V. 2012. Identification of acquired antimicrobial resistance genes. J Antimicrob Chemother 67:2640–2644.

4. Redgrave LS, Sutton SB, Webber MA, Piddock LJV. 2014. Fluoroquinolone resistance: mechanisms, impact on bacteria, and role in evolutionary success. Trends Microbiol 22:438–445.

5. Lesher GY, Froelich EJ, Gruett MD, Bailey JH, Brundage RP. 1962. 1,8-Naphthyridine Derivatives. A New Class of Chemotherapeutic Agents. J Med Pharm Chem 5:1063–1065.

6. Andriole VT. 2005. The quinolones: past, present, and future. Clin Infect Dis 41 Suppl 2:S113-9.

7. Emmerson AM, Jones AM. 2003. The quinolones: decades of development and use. J

Antimicrob Chemother 51:13–20.

8. Levine C, Hiasa H, Marians KJ. 1998. DNA gyrase and topoisomerase IV: biochemical activities, physiological roles during chromosome replication, and drug sensitivities. Biochim Biophys Acta 1400:29–43.

9. Ruiz J. 2003. Mechanisms of resistance to quinolones: target alterations, decreased accumulation and DNA gyrase protection. J Antimicrob Chemother 51:1109–17.

10. Hooper DC. 1999. Mechanisms of fluoroquinolone resistance. Drug Resist Updat 2:38–55.

11. Shen LL, Mitscher LA, Sharma PN, O 'donnel1 TJ, Chu DWT, Cooper CS, Rosen T, Pernett AG. 1989. Mechanism of Inhibition of DNA Gyrase by Quinolone Antibacterials: A Cooperative Drug-DNA Binding Model. Biochemistry 28:3886–3894.

12. Hooper DC, Jacoby GA. 2015. Mechanisms of drug resistance: quinolone resistance. Ann N Y Acad Sci 1354:12–31.

13. Martínez-Martínez L, García I, Ballesta S, Benedí VJ, Hernández-Allés S, Pascual A. 1998. Energy-dependent accumulation of fluoroquinolones in quinolone-resistant *Klebsiella pneumoniae* strains. Antimicrob Agents Chemother 42:1850–2.

14. Martínez-Martínez L, Pascual A, Conejo M del C, García I, Joyanes P, Doménech-Sánchez A, Benedí VJ. 2002. Energy-dependent accumulation of norfloxacin and porin expression in clinical isolates of *Klebsiella pneumoniae* and relationship to extended-spectrum beta-lactamase production. Antimicrob Agents Chemother 46:3926–32.

15. Mazzariol A, Zuliani J, Cornaglia G, Rossolini GM, Fontana R. 2002. AcrAB Efflux

System: Expression and Contribution to Fluoroquinolone Resistance in *Klebsiella* spp. Antimicrob Agents Chemother 46:3984–3986.

16. Schneiders T, Amyes SGB, Levy SB. 2003. Role of AcrR and RamA in Fluoroquinolone Resistance in Clinical *Klebsiella pneumoniae* Isolates from Singapore Role of AcrR and RamA in Fluoroquinolone Resistance in Clinical *Klebsiella pneumoniae* Isolates from Singapore 47:2831–2837.

17. Veleba M, Higgins PG, Gonzalez G, Seifert H, Schneiders T. 2012. Characterization of RarA, a novel AraC family multidrug resistance regulator in *Klebsiella pneumoniae.* Antimicrob Agents Chemother 56:4450–4458.

18. Sørensen AH, Hansen LH, Johannesen E, Sørensen SJ. 2003. Conjugative plasmid conferring resistance to olaquindox. Antimicrob Agents Chemother 47:798–9.

19. Hansen LH, Johannesen E, Burmolle M, Sorensen AH, Sorensen SJ. 2004. Plasmid-Encoded Multidrug Efflux Pump Conferring Resistance to Olaquindox in *Escherichia coli*. Antimicrob Agents Chemother 48:3332–3337.

20. Martínez-Martínez L, Pascual A, Jacoby GA. 1998. Quinolone resistance from a transferable plasmid. Lancet (London, England) 351:797–9.

21. Jacoby GA, Walsh KE, Mills DM, Walker VJ, Oh H, Robicsek A, Hooper DC. 2006. qnrB, another plasmid-mediated gene for quinolone resistance. Antimicrob Agents Chemother 50:1178–82.

22. Wang M, Guo Q, Xu X, Wang X, Ye X, Wu S, Hooper DC, Wang M. 2009. New plasmid-mediated quinolone resistance gene, qnrC, found in a clinical isolate of *Proteus mirabilis*. Antimicrob Agents Chemother 53:1892–7.

23. Hata M, Suzuki M, Matsumoto M, Takahashi M, Sato K, Ibe S, Sakae K. 2005. Cloning of a novel gene for quinolone resistance from a transferable plasmid in *Shigella flexneri* 2b. Antimicrob Agents Chemother 49:801–3.

24. Cavaco LM, Hasman H, Xia S, Aarestrup FM. 2009. qnrD, a Novel Gene Conferring Transferable Quinolone Resistance in *Salmonella enterica* Serovar Kentucky and Bovismorbificans Strains of Human Origin. Antimicrob Agents Chemother 53:603–608.

25. Robicsek A, Strahilevitz J, Jacoby GA, Macielag M, Abbanat D, Hye Park C, Bush K, Hooper DC. 2006. Fluoroquinolone-modifying enzyme: a new adaptation of a common aminoglycoside acetyltransferase. Nat Med 12:83–88.

26. George AM, Hall RM, Stokes HW. 1995. Multidrug resistance in *Klebsiella pneumoniae*: a novel gene, ramA, confers a multidrug resistance phenotype in *Escherichia coli*. Microbiology 141 (Pt 8:1909–20.

27. De Majumdar S, Yu J, Fookes M, McAteer SP, Llobet E, Finn S, Spence S, Monahan A, Monaghan A, Kissenpfennig A, Ingram RJ, Bengoechea J, Gally DL, Fanning S, Elborn JS, Schneiders T. 2015. Elucidation of the RamA regulon in *Klebsiella pneumoniae* reveals a role in LPS regulation. PLoS Pathog 11:e1004627.

28. Clinical and Laboratory Standards Institute. 2006. M2-A9. Performance Standards for Antimicrobial Disc Susceptibility Tests Approved Standard – Ninth Edition. CLSI, Wayne, PA, USA.

29. Clinical and Laboratory Standards Institute. 2015. M07-A10 Methods for Dilution Antimicrobial Susceptibility Tests for Bacteria That Grow Aerobically; Approved

Standard—Tenth Edition. CLSI, Wayne, PA, USA.

30. Clinical and Laboratory Standards Institute. 2015. M100-S25 Performance Standards for Antimicrobial Susceptibility Testing; Twenty-Fifth Informational Supplement An informational supplement for global application developed through the Clinical and Laboratory Standards Institute consensus process. CLSI, Wayne, PA, USA.

31. Jiménez-Castellanos J-C, Wan Ahmad Kamil WNI, Cheung CHP, Tobin MS, Brown J, Isaac SG, Heesom KJ, Schneiders T, Avison MB. 2016. Comparative effects of overproducing the AraC-type transcriptional regulators MarA, SoxS, RarA and RamA on antimicrobial drug susceptibility in *Klebsiella pneumoniae*. J Antimicrob Chemother 71:1820–1825.

32. Jiménez-Castellanos J-C, Wan Nur Ismah WAK, Takebayashi Y, Findlay J, Schneiders T, Heesom KJ, Avison MB. 2017. Envelope proteome changes driven by RamA overproduction in *Klebsiella pneumoniae* that enhance acquired β-lactam resistance. J Antimicrob Chemother. doi: 10.1093/jac/dkx345. [Epub ahead of print].

33. Silva JC, Gorenstein M V, Li G-Z, Vissers JPC, Geromanos SJ. 2006. Absolute quantification of proteins by LCMSE: a virtue of parallel MS acquisition. Mol Cell Proteomics 5:144–56.

34. Coldham NG, Webber M, Woodward MJ, Piddock LJ V. 2010. A 96-well plate fluorescence assay for assessment of cellular permeability and active efflux in *Salmonella enterica serovar Typhimurium* and *Escherichia coli*. J Antimicrob Chemother 65:1655–63.

35. Bolger AM, Lohse M, Usadel B. 2014. Trimmomatic: a flexible trimmer for Illumina

sequence data. Bioinformatics 30:2114–2120.

36. Carattoli A, Zankari E, Garcia-Fernandez A, Voldby Larsen M, Lund O, Villa L, Moller Aarestrup F, Hasman H. 2014. In Silico Detection and Typing of Plasmids using PlasmidFinder and Plasmid Multilocus Sequence Typing. Antimicrob Agents Chemother 58:3895–3903.

37. Zankari E, Hasman H, Cosentino S, Vestergaard M, Rasmussen S, Lund O, Aarestrup FM, Larsen MV. 2012. Identification of acquired antimicrobial resistance genes. J Antimicrob Chemother 67:2640-4.

38. Darling AE, Mau B, Perna NT, Batzoglou S, Zhong Y. 2010. progressiveMauve: Multiple Genome Alignment with Gene Gain, Loss and Rearrangement. PLoS One 5:e11147.

39. Su C-C, Rutherford DJ, Yu EW. 2007. Characterization of the multidrug efflux regulator AcrR from *Escherichia coli*. Biochem Biophys Res Commun 361:85–90.